

Selection of efficient earthquake intensity measures for evaluating seismic fragility of concrete face rockfill dam

Muhammad Irsfan Khalid^a, Duhee Park^b, Jianbo Fei^{a,*}, Van-Quang Nguyen^{b,c,*},
Duy-Duan Nguyen^c, Xiangsheng Chen^a

^a Key Laboratory of Coastal Urban Resilient Infrastructures, College of Civil and Transportation Engineering, Shenzhen University, Shenzhen 518060, China

^b Department of Civil and Environment Engineering, Hanyang University, 222, Wangsimni-ro, Seongdong-gu, Seoul, 04763, Republic of Korea

^c Department of Civil Engineering, Vinh University, Vinh 461010, Viet Nam

ARTICLE INFO

Keywords:

Concrete face rockfill dam
Seismic fragility analysis
Ground motion intensity measure
Probabilistic seismic demand model
Damage index

ABSTRACT

This study explores the crucial role of intensity measure (IM) selection for probabilistic seismic demand model development of concrete face rockfill dam (CFRD) subjected to earthquake ground motions. Nonlinear dynamic analyses are performed for CFRD with an advanced hysteretic soil model using a finite element analysis program to develop a database of earthquake-induced dam crest settlements. The numerical model is validated through centrifuge model test measurements. A selection process was carried out to evaluate the IMs based on the goodness of fit, as well as their efficiency, practicality, and proficiency. Eventually, a range of optimal IMs are selected. Conditional probability function is employed to develop fragility curves for CFRD employing both scalar and vector IMs. Five settlement ratio-based limit states are defined herein. The results show that vector fragility surfaces produce enhanced predictions of the dam damage compared with the scalar fragility curves that are most often employed.

1. Introduction

The concrete face rockfill dam (CFRD) is becoming a more and more common type of dam. It is because of its exceptional seismic resistance, adaptability to various geological and hydrological conditions, and adequate use of local materials [Cooke, 1992; Ma and Chi, 2016; Xing et al., 2006]. Although the damage to CFRDs in recent strong earthquakes is manageable [Shannon, 2009; Xu, 2008; Yamaguchi et al., 2008; Zhang et al., 2010], the public remains very concerned about the potential risk of seismic consequences. It is necessary to carefully evaluate the seismic performance of CFRDs.

Seismic damage and fragility analyses of dams were extensively researched [Huang et al., 2023; Li et al., 2021; Li et al., 2022; Liang et al., 2020; Mahmoodi et al. (2021); Pang et al., 2018a; Segura et al., 2020; Sevieri et al., 2021; Sun et al. (2022); Tidke and Adhikary, 2021; Wang et al., 2018]. However, few studies have been conducted on CFRDs. Pang et al. (2018b) introduced an incremental dynamic analysis-based seismic fragility analysis approach for evaluating the seismic performance of high CFRDs. The permanent deformation of the dam crest and damage index of face-slabs were used to define damage states.

The peak ground acceleration (PGA) was selected as the earthquake motion intensity measure (IM) to develop fragility curves. Pang et al. (2020) investigated the effect of aftershocks on the fragility of high CFRDs. The engineering demand parameter (EDP) was selected among the deformation, shear strain, and damage index of the face slabs. The PGA was used to construct the fragility curves of the CFRD under different seismic conditions. Zhou et al. (2021) performed the seismic fragility of a high CFRD by combining the finite element method (FEM) and machine learning (i.e., SVM: support vector machine). FEM was used to generate a dataset, while SVM was employed to train the relationship between the IMs and EDPs. The results highlighted that PGA is an optimal earthquake IM to develop the seismic fragility curves among cumulative absolute velocity (CAV), Arias intensity (I_a), and predominant period (T_p). Xu et al. (2022) investigated the effect of multi-components strong motion duration on seismic performance of high CFRDs. To develop fragility curves, the relative settlement ratio (SR) (i.e., crest settlement/dam height) of the dam crest and the PGA was considered as an EDP and an earthquake IM, respectively. The previous studies mostly used PGA or less earthquake IM to construct the fragility curves. A comprehensive study to optimal earthquake IMs for developing fragility curves of CFRDs is needed.

* Corresponding authors.

E-mail addresses: feijianbo@szu.edu.cn (J. Fei), nguyenvanquang240484@gmail.com (V.-Q. Nguyen).

Nomenclature			
IM	intensity measure	P_f	probability function
CFRD	concrete face rockfill dam	Φ	cumulative distribution function
EDP	engineering demand parameter	$\sigma_{EDP/IM}$	standard deviation
FEM	finite element method	SR	crest settlement ratio
SVM	support vector machine	R^2	linear regression coefficient
DRLF	dam reservoir layered foundation	b	practicality coefficient
M_w	moment magnitude	ξ	modified dispersion
R_{rup}	rupture distance	DI	damage index
EDOF	equal degree of freedom	GQ/H	generalized quadratic/hyperbolic
V_s	shear wave velocity	σ_c	confining pressure
PSDM	probabilistic seismic demand model	f_{max}	maximum frequency
		ECRD	earth core rockfill dam

Optimization of earthquake IMs for developing fragility curves was widely studied in many structures, such as buildings [Kazantzi and Vamvatsikos, 2015; Kostinakis et al., 2015; Macabuag et al., 2016; Nguyen et al., 2023; Pejovic et al., 2017; Pejovic et al., 2018; Rong et al., 2023], bridges [Guo et al., 2020; Hu et al., 2022; Wei et al., 2020; Zelaschi et al., 2019; Zhang and Huo, 2009], tunnels [Huang et al., 2021; Sun et al., 2023], and nuclear power plant structures [Li et al., 2019; Nguyen et al., 2021; Nguyen et al., 2020]. There are several studies that have been done on dams. Hariri-Ardebili and Saouma (2016) developed a relationship between 70 IMs and EDP (i.e., crest displacement) for concrete dams. It was reported that the spectral acceleration at the fundamental period of the structure is an optimal IM for developing fragility curves. Padgett et al. (2008) evaluated optimal intensity measures (IMs) for the seismic fragility analysis of the dam-reservoir-layered foundation (DRLF) system. They concluded that acceleration spectrum intensity (ASI) and effective design acceleration (EDA) are observed to have excellent predictability and show the best correlation for the considered EDPs of the dam. The literature review demonstrated that a study developing a relationship between IMs and EDP has not yet been performed for CFRDs.

This study aims to identify optimal IMs to develop probabilistic seismic demand models (PSDMs) of CFRDs. For that, 20 earthquake IMs are considered in developing PSDMs. The nonlinear numerical modeling of CFRD is constructed using hysteretic and elastic models for soil and concrete in LS-Dyna program [LSTC, 2007]. A set of 100 ground motion records, which contain a wide range of amplitudes, magnitudes, epicentral distances, significant durations, and predominant periods, are utilized to perform nonlinear time history analyses. Optimal IMs are evaluated based on statistical indicators of PSDMs, which are the coefficient of determination, dispersion, practicality, and proficiency. Finally, seismic fragility curves of CFRDs with respect to optimal IMs are drawn. In addition, seismic fragility surfaces for vector IMs are developed (i.e., the PGA and PGV simultaneously).

2. Earthquake intensity measures and input ground motions

2.1. Earthquake intensity measures

Earthquake IMs are critical for representing the crucial properties of seismic motion compactly and quantitatively. Numerous IMs have been proposed to describe the amplitude, frequency content, and duration of motions [Kramer, 1996]. The seismic IMs can be calculated using software or directly from earthquake accelerograms. This study takes into consideration a total of 20 typical earthquake IMs, and SeismoSignal [Seismosoft, 2012] is used to determine these parameters for each ground motion. The used IMs are listed in Table 1.

Table 1
20 earthquake intensity measures.

No.	Intensity measure (unit)	Notation	Reference
1	Peak ground acceleration (g)	PGA	Kramer (1996)
2	Peak ground velocity (m/s)	PGV	Kramer (1996)
3	Peak ground displacement (m)	PGD	Kramer (1996)
4	Ratio of PGV to PGA (s)	PGV/ PGA	Kramer (1996)
5	Root-mean-square of acceleration (g)	A_{rms}	Housner and Jennings (1964)
6	Root-mean-square of velocity (m/s)	V_{rms}	Housner and Jennings (1964)
7	Root-mean-square of displacement (m)	D_{rms}	Housner and Jennings (1964)
8	Arias intensity (m/s)	I_a	Arias (1970)
9	Characteristic intensity ($m^{1.5}/s^{2.5}$)	I_c	Park et al. (1985)
10	Specific energy density (m^2/s)	SED	–
11	Cumulative absolute velocity (m/s)	CAV	Kramer (1996)
12	Acceleration spectrum intensity (g^*s)	ASI	Housner (1952)
13	Velocity spectrum intensity (m)	VSI	Housner (1952)
14	Housner spectrum intensity (m)	HI	Housner (1952)
15	Sustained maximum acceleration (g)	SMA	Nuttl (1979)
16	Sustained maximum velocity (m/s)	SMV	Nuttl (1979)
17	Effective design acceleration (g)	EDA	Benjamin (1988)
18	A95 parameter (g)	A_{95}	Sarma and Yang (1987)
19	Predominant period (s)	T_p	Kramer (1996)
20	Mean period (s)	T_m	Rathje et al. (1998)

2.2. Input ground motion

A total of 100 earthquake ground motions are selected from the NGA-west2 database (<https://ngawest2.berkeley.edu/>). Ground motions are chosen based on a wide range of earthquake amplitudes, magnitudes, epicentral distances, significant durations, and predominant periods. The acceleration response spectra and PGA-rupture distance (R_{rup})-moment magnitude (M_w) of selected motions are present in Fig. 1 and Fig. 2.

3. Concrete face rockfill dam (CFRD) modeling

This section presents the finite element analysis approach for CFRD using the commercial FE program LS-DYNA to simulate the non-linear response of CFRD. The dynamic equation of motion is solved using the explicit central difference time integration scheme. The centrifuge test measurements and calculated numerical simulation results of CFRD are compared.

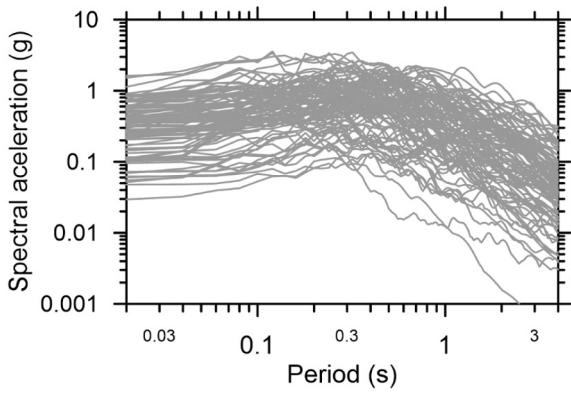


Fig. 1. Acceleration response spectra.

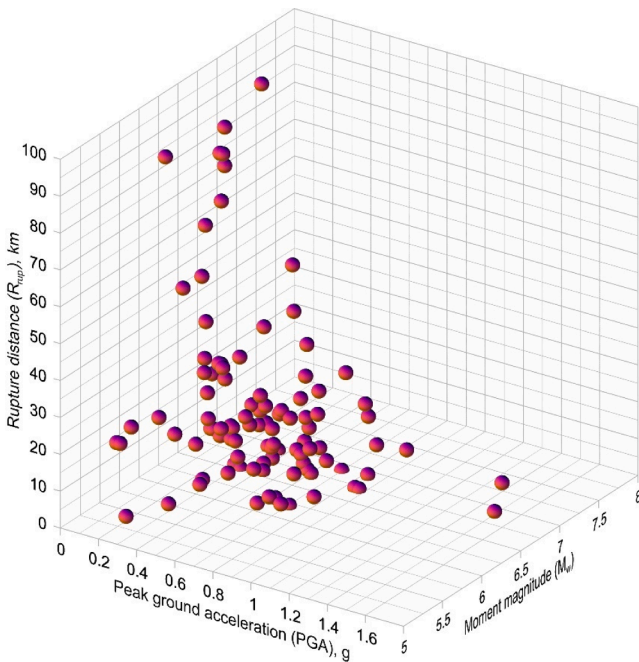


Fig. 2. PGA- R_{rup} - M_w distribution of input ground motions.

3.1. Numerical model of CFRD

In this study, the finite element analysis program LS-Dyna [LSTC, 2007] was used as a simulation tool. The 2D dynamic analyses of the concrete face rockfill dam (CFRD) were performed to measure the settlement at the crest. In this study, the standard section of the CFRD in Korea was used. The standard section of the dam with a width of 185 m and a height of 60 m was used. The upstream and the downstream slope is 1:1.4. The numerical analysis model of CFRD is depicted in Fig. 3. For

the simulation of the free field boundary condition, the equal degree of freedom constraint (EDOF) was applied. The prescribed boundary condition was applied on the base nodes to simulate the rigid base. The base nodes were fixed vertically and allowed to move in the horizontal direction.

The four-node plane strain elements were selected for the discretization of the soil domain. The pre-earthquake stresses were modeled carefully because the state of stress affects the shear strength and the initial conditions for dynamic analysis. The inclined layers were produced along the slope to account for confining pressure dependency of shear wave velocity (V_s) [Khalid et al. (2021a); Lee et al., 2020]. The average value of soil properties of leading dams in Korea was applied in the numerical model of the dam [Baeg et al., 2018]. A shear wave velocity profile shown in Fig. 4 was used in the simulation. The static water pressure was exerted on the concrete face slab during the dynamic analysis. The element size was selected such as to propagate the motion frequencies accurately, as recommended by Kuhlemeyer and Lysmer (1973). The height of element was set to 0.5 m to transmit a minimum of 25 Hz components using the following equation (1):

$$H = \frac{V_s}{4f_{max}} \tag{1}$$

where H is the element height, V_s is the shear wave velocity, and f_{max} is the max frequency of ground motion.

The seismic response of slopes is affected by the nonlinear behavior of soil. In this study, the elasto-plastic hysteretic soil model (MAT-079 in

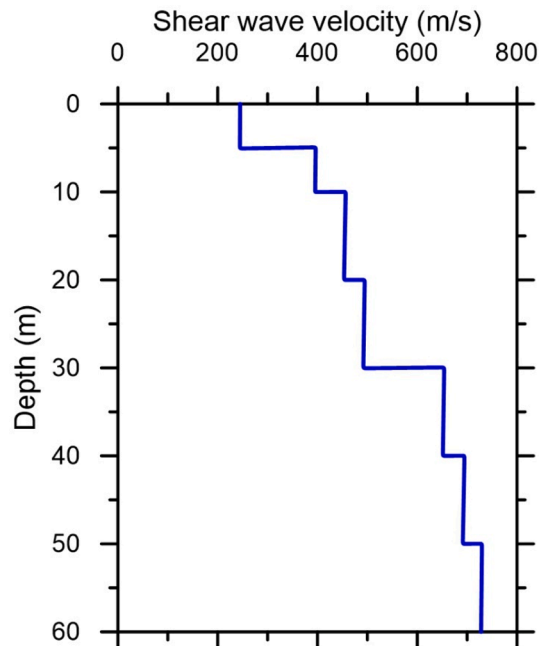


Fig. 4. Shear wave velocity profile.

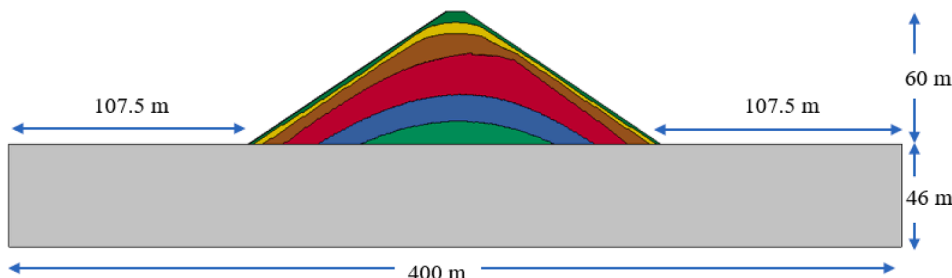


Fig. 3. Numerical Model of CFRD, in which different soil layers are represented by various colors.

the library of LS-Dyna), which is one of the widely used nonlinear soil models in seismic computation, was used to simulate nonlinear soil response. The nonlinear soil model is a nested elastic-perfectly plastic yield surface model that incorporates the pressure-dependent shear strength of the soil [Bolisetti et al., 2018; Hashash et al., 2018; Khalid et al. (2021b); LSTC, 2007].

The properties of the nonlinear soil model were incorporated through shear strength curves, which were developed for each layer through modulus reduction and damping curves of Darendeli [Darendeli, 2001]. The curves were fitted with Darendeli [Darendeli, 2001], and shear strength correction was applied as recommended by Lee et al. (2020), because the settlement of the crest is affected by shear strength correction. The GQ/H (generalized quadratic/hyperbolic) model was used for shear strength correction, which achieves the target shear strength at large strains and follows the modulus reduction curves up to a shear strain of 0.1% [Groholski et al., 2016]. In addition, the model requires the bulk modulus and mass density of the material. Shear stress-strain curves for selected soil layers at different confining pressure are also shown in Fig. 5. The hysteretic behavior of soil was incorporated through the Masing rule. The frequency-independent damping formulation was applied to all components of the numerical model to model small strain damping.

3.2. Validation of the numerical model

In this study, the numerical model is validated through the centrifuge measurements performed in Korean Advanced Institute of Science and Technology (KAIST). KAIST beam centrifuge has an effective radius of 5.0 m and a maximum capacity of 2400 kg. Kim et al. (2011) performed the centrifuge model tests for two types of Korean dams: ECRD and CFRD. To validate the numerical model, we used the measured data of CFRD. The upstream and downstream slope of the CFRD model was 1:1.4. The centrifuge test was performed at a centrifugal acceleration of 40 g. The height of the dam in a prototype scale is 6.4 m, and in the centrifuge model is 160 mm. The dam model was constructed directly on the baseplate of the model container. It is because the CFRD dams are mostly constructed on the top of bedrock in Korea. Fig. 6 shows the location of accelerometers and strain gages in the centrifuge model to measure dam response to the earthquake.

Fig. 7 shows the numerical model used for validation. The centrifuge test performed in a significantly small scale can represent the dam behavior in the actual size. Thus, the centrifuge measurements were considered acceptable for validating the numerical model [Kim et al., 2011]. Resonant column tests were performed to give the relationship between confining pressure and shear velocity. Kim et al. (2011) proposed the following equation based on the results of resonant column tests.

$$V_s = 100.4 * (\sigma_c)^{0.24} \tag{2}$$

where V_s is shear wave velocity (m/s) and σ_c is confining pressure (kPa).

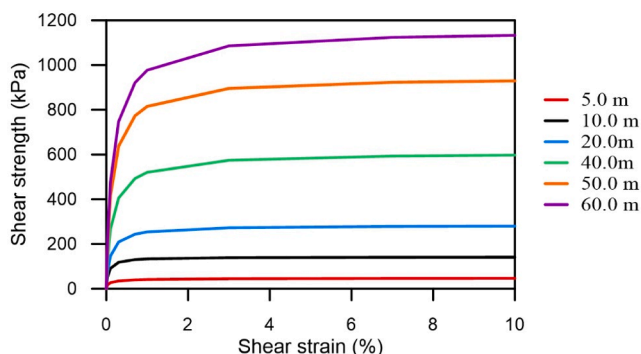


Fig. 5. Shear stress versus strain curves.

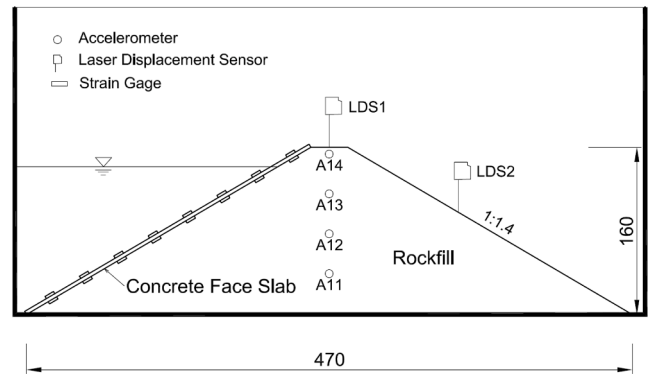


Fig. 6. Centrifuge model of concrete face rockfill dam [Kim et al., 2011].

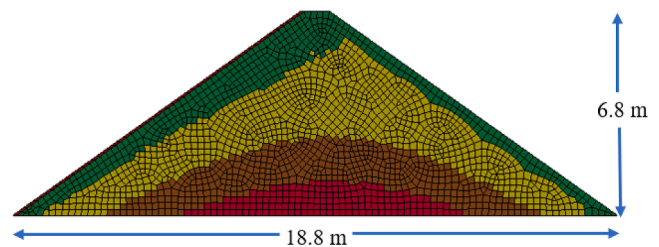


Fig. 7. Numerical model for validation.

The numerical model is similar to the CFRD model presented earlier in the previous section.

Acceleration time history and 5% damped response spectra of input motion are shown in Fig. 8. The input motion selected for comparison has a PGA of 0.166 g. The measured values by Kim et al. (2011) are compared with calculated response spectra in finite element analysis. The results of accelerometers A11, A12, A13, and A14 are depicted in Fig. 9. It is illustrated that the measured acceleration response spectra fit well with the calculated data. The comparison results show that calculated and measured response spectra produce peaks at approximately the same periods. Thus, we conclude that the numerical model shows a reliable estimate of the response spectra of the dam.

4. Regression between EDP and IMs

The estimation of earthquake-induced dam displacement is much the same problem as the estimation of structural response, in both cases, the objective is the estimation of seismic effects on a system instead of the estimation of ground motions alone as is done in probabilistic seismic hazard analyses. In the past few years, many researchers have worked on the probabilistic evaluation of structural response. This study has been commonly performed based on performance-based earthquake engineering. In this regard, the structural response is estimated by engineering demand parameters (EDPs) which are estimated by earthquake ground motion intensity measures (IMs). In the case of dam slopes, earthquake-induced crest settlements act as an engineering demand parameter in structural response.

A series of nonlinear time history analyses were performed on the dam. The input ground motions were applied to the base of the dam model in the horizontal direction. The seismic response of the dam slope is obtained in terms of the maximum crest settlement and acceleration time history at the crest.

4.1. Probabilistic seismic demand model (PSDM)

A relationship is developed to identify the weak and strong correlation between the seismic response of dam slope quantified by EDP and

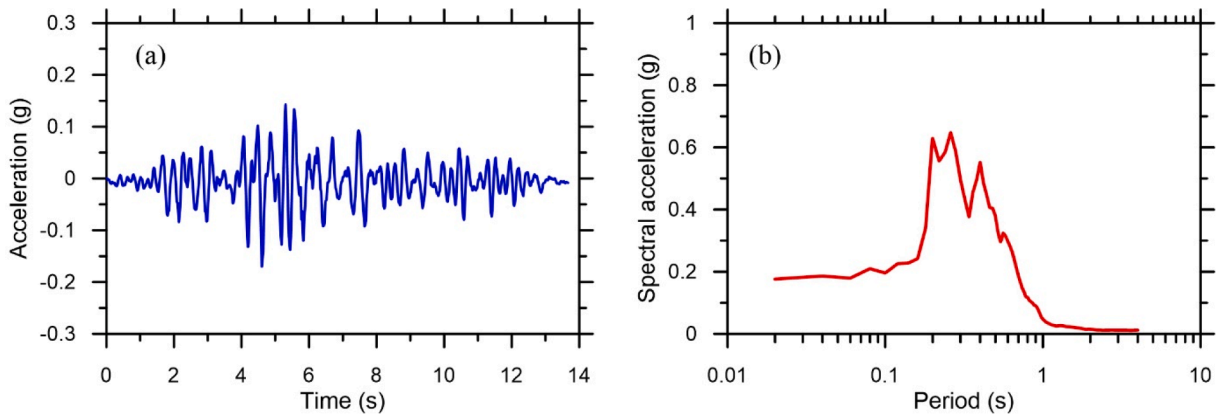


Fig. 8. Input motion (a) Acceleration time history (b) Response spectra.

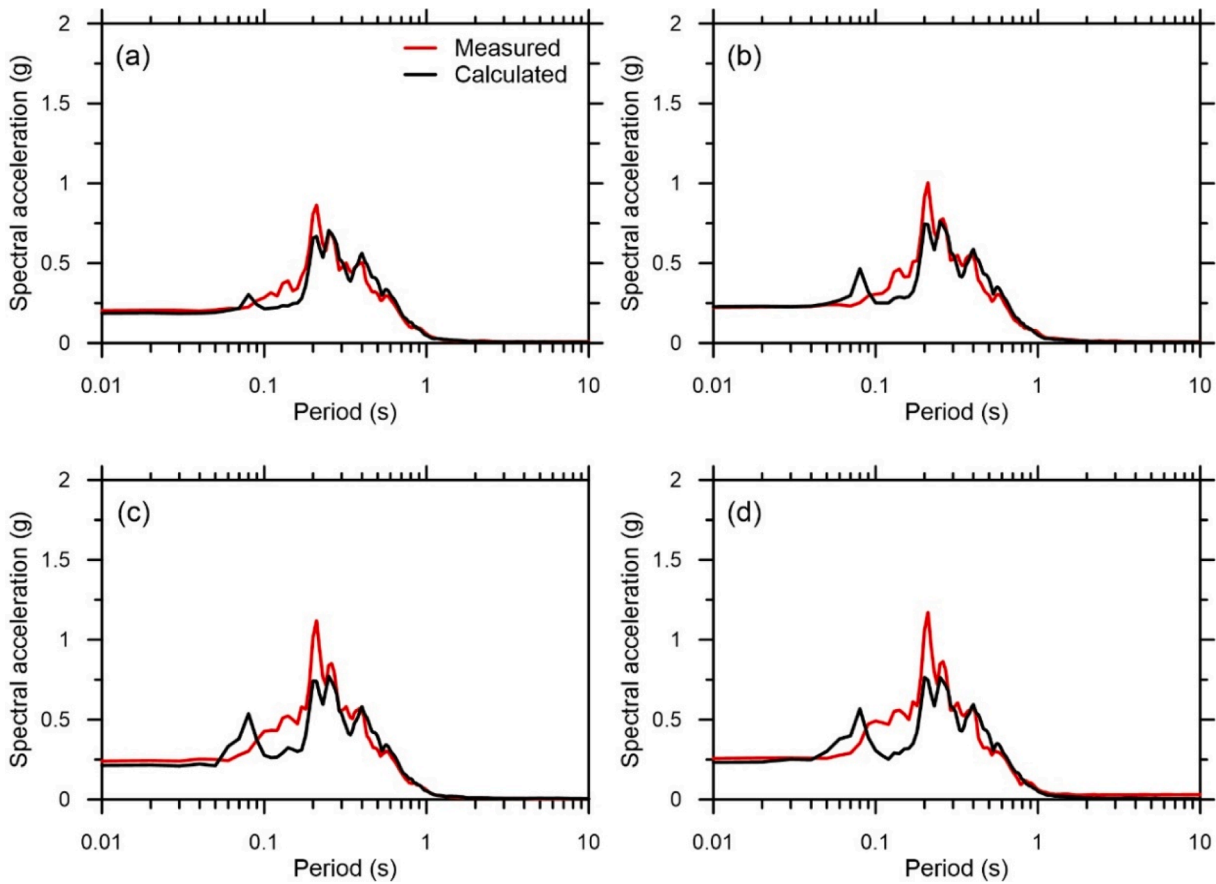


Fig. 9. Comparison of the measured and calculated acceleration response spectra (a) A11 (b) A12 (c) A13 (d) A14.

earthquake ground motion intensity measures (IMs). The relationship between EDP and IMs is as follows [Cornell et al., 2002; Hu et al., 2020; Lee et al., 2019]:

$$EDP = a*(IM)^b \tag{3}$$

The natural logarithm is taken on equation (3) and assumed the distribution of the seismic demand to be lognormal distributed [Lu et al., 2015; Mackie and Stojadinović, 2001]:

$$\ln(EDP) = \ln(a) + b*\ln(IM) \tag{4}$$

The probabilistic seismic demand model (also known as fragility function) is a common and essential step for performance-based earthquake engineering of the dam, which is a relationship between the dam

response (crest settlement ratio (SR)) and the intensity measure of earthquake motion. In this approach, the fragility function is a conditional probability function showing the probability that the dam experiences a specific damage level for a given level of earthquake motion intensity.

$$P_f = P[EDP \geq C|IM] \tag{5}$$

This conditional probability function is assumed to follow a log-normal distribution function, as expressed by

$$P[EDP \geq C|IM] = 1 - \Phi \left[\frac{\ln(a*(IM)^b) - \ln(C)}{\sigma_{EDP|IM}} \right] \tag{6}$$

where $(P[EDP \geq C|IM])$ is the probability, and Φ is the cumulative distribution function of the normal distribution. The standard deviation $\sigma_{EDP|IM}$ is obtained from the nonlinear time history analyses, as shown in

equation (7):

$$\sigma_{EDP|IM} = \sqrt{\frac{\sum (\ln(d_i) - \ln(a \times IM^b))^2}{n - 2}} \tag{7}$$

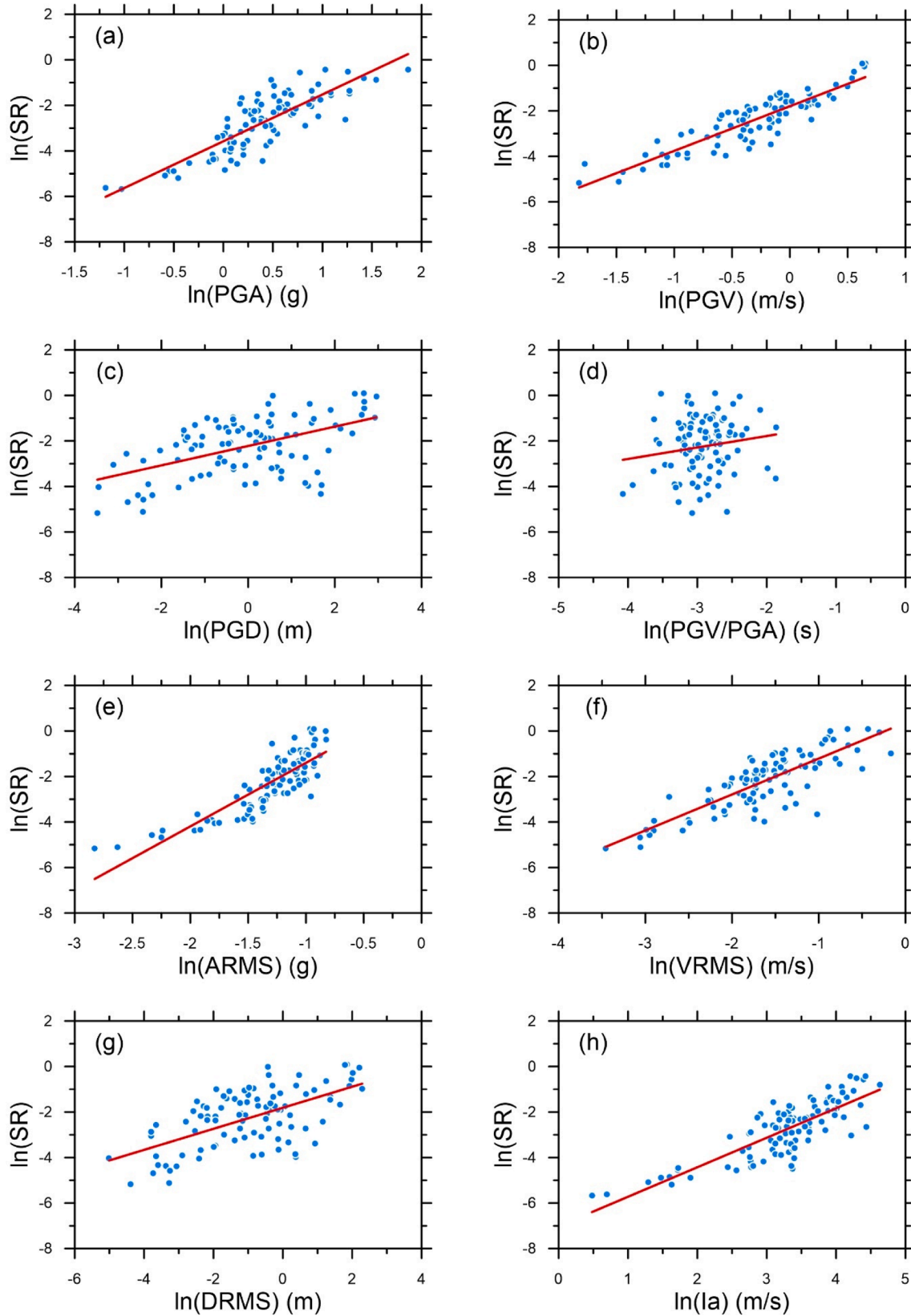


Fig. 10. Calculated settlement ratio vs IMs in logarithmic scale.

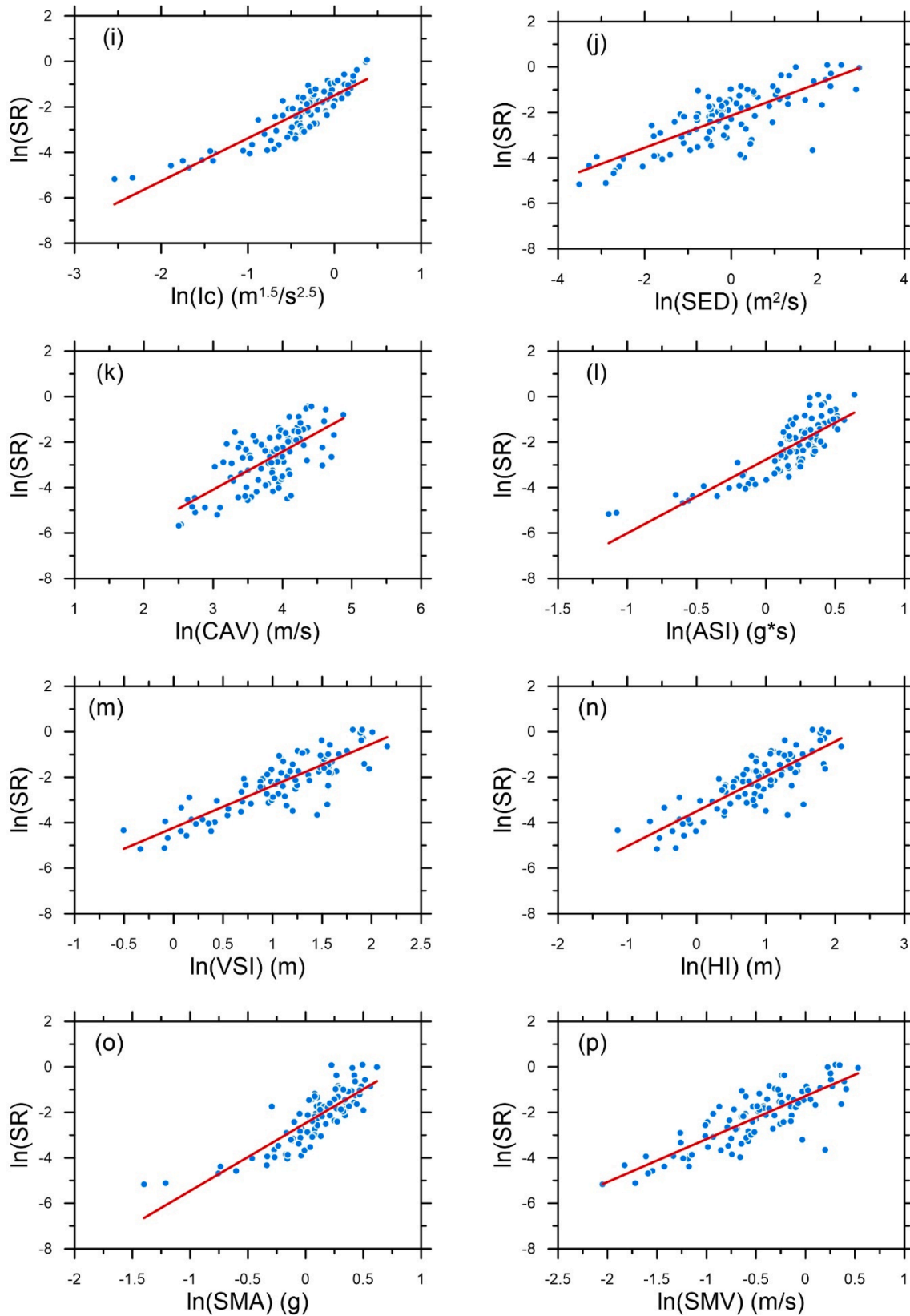


Fig. 10. (continued).

where n is the total number of ground motions, and d_i is the individual result of the nonlinear time history analyses.

4.2. Correction between the settlement ratio and IMs

Blue dots in Fig. 10 are the representative results of the calculated settlement ratio and 20 IMs calculated from acceleration time history at

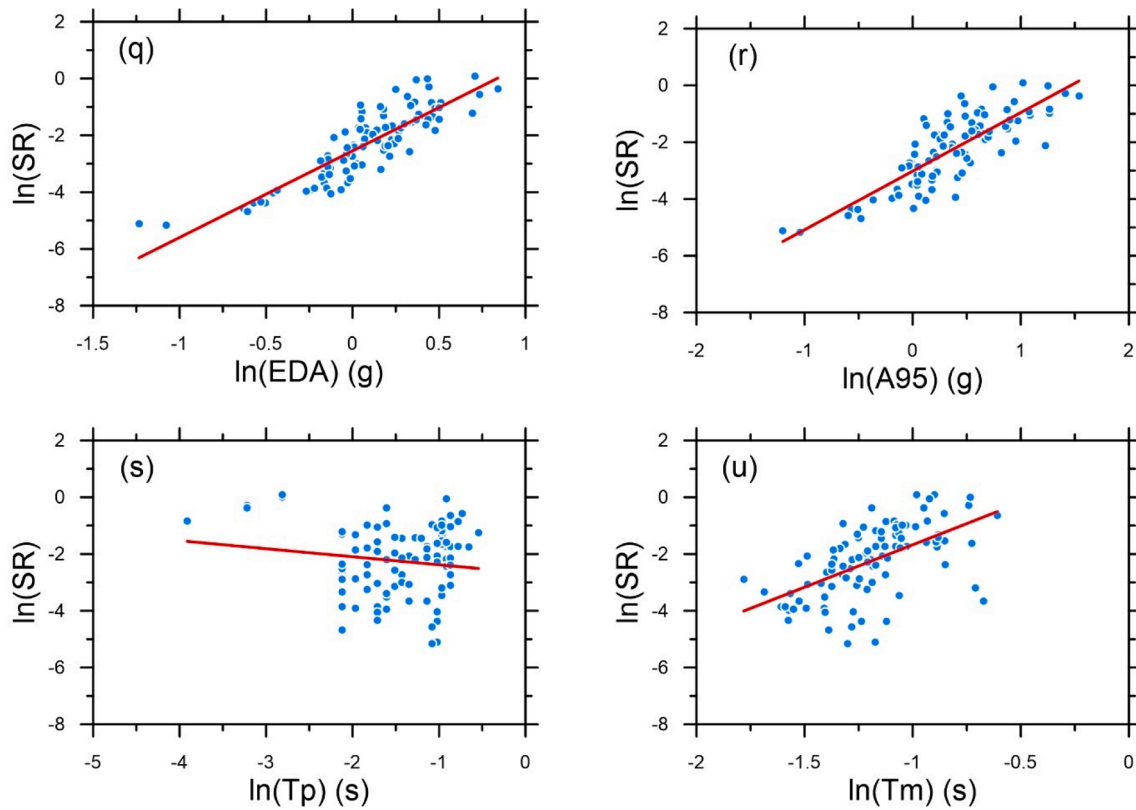


Fig. 10. (continued).

the crest. The two coefficients of linear regressions were estimated using the results of time history analyses (crest settlement ratio (SR)) and corresponding to the given intensity measures of the ground motions, described in equation (4). Red lines in Fig. 10 depict the fitted correlations between the settlement ratio and various earthquake IMs.

4.3. Optimal IM selection

Given the 20 intensity measures, an important question arises: which is the optimal intensity measure for predicting dam settlement? This section examines the optimal intensity measure considering settlement ratio as the EDP for concrete face rockfill dams in PSDMs. The goodness of fit, efficiency, practicality, and proficiency are evaluated to judge the optimal IMs.

4.3.1. Goodness of fit

The goodness of fit is a well-accepted and good indicator of data fitting. In the probabilistic seismic demand model (PSDM), the linear regression coefficient (R^2) is used to determine the goodness of fit. The regression coefficient depicts the discrepancy between the measured data and the fitted regression line. The value of the regression coefficient can range from 0 to 1. The more precise the prediction of the data trend and less scatter as closer the data regression coefficient is to one.

The goodness of fit of the IMs is determined for linear regression of the PSDM in the logarithmic space and presented in Fig. 11. The value of goodness of fit is close to one, the more good is the approximation between IM and EDP. As shown in Fig. 11, PGV achieved the highest R^2 value ($R^2 = 0.81$), followed by I_c ($R^2 = 0.79$) and EDA ($R^2 = 0.75$). In contrast, PGV/PGA showed a relatively small R^2 value ($R^2 = 0.02$).

4.3.2. Efficiency

The efficiency is mostly examined criterion for selecting optimal IMs. The variation and dispersion of seismic demand predictions for a ground motion IM are decreased by an efficient IM [Giovenale et al., 2004]. The

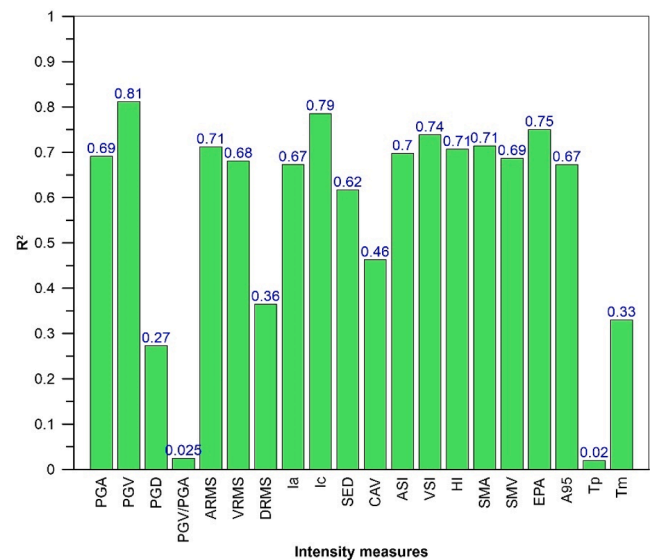


Fig. 11. Correlation coefficient (R^2).

nonlinear time history analysis results are used to investigate the IM efficiency through the standard deviation ($\sigma_{EDP/IM}$), which is described in equation (7). The efficiency is inversely proportional to the standard deviation ($\sigma_{EDP/IM}$). The lower efficiency of IM corresponds to higher standard deviation.

The efficiencies of different IMs can be determined using $\sigma_{EDP/IM}$ calculated through equation (7). The lower the value of $\sigma_{EDP/IM}$, the more efficient the IM, and higher values indicate less efficient IM. As shown in Fig. 12, the highest efficiency, denoted by $\sigma_{EDP/IM}$, belongs to PGV ($\sigma_{EDP/IM} = 0.52$). In addition, I_c ($\sigma_{EDP/IM} = 0.56$), EDA ($\sigma_{EDP/IM} = 0.61$),

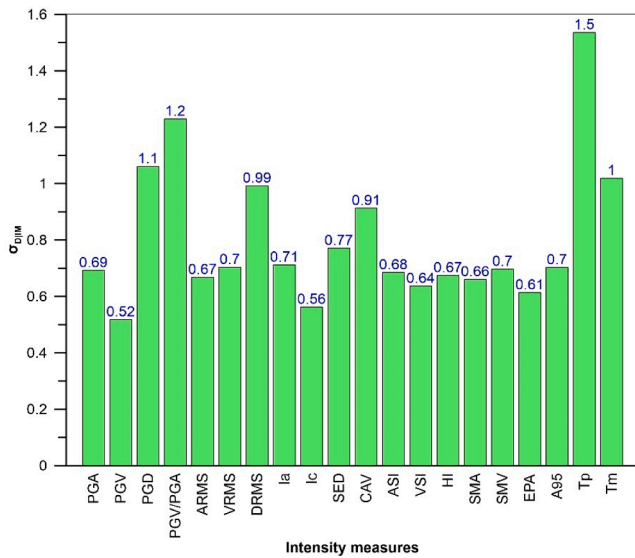


Fig. 12. The $\sigma_{EDP/IM}$ values for efficiency.

ARMS and SMA ($\sigma_{EDP/IM} = 0.66$) provided the greatest appropriate efficiency and were the most efficient IMs followed by PGV. The maximum standard deviation ($\sigma_{EDP/IM}$) is observed for T_p ($\sigma_{EDP/IM} = 1.54$), highlighting that this IM is the least efficient followed by PGV/PGA ($\sigma_{EDP/IM} = 1.23$), PGD ($\sigma_{EDP/IM} = 1.06$) and T_m ($\sigma_{EDP/IM} = 1.02$).

4.3.3. Practicality

The practicality criterion reveals that the intensity measure and the resulting EDP have a direct relationship. The amount of EDP has minimal to no dependence on the magnitude of the seismic intensity measure if an intensity measure is not practical. An IM-EDP pair in a PSDM is practical if it is easy to construct from readily available ground motion IMs and nonlinear analysis response values and makes sense from an engineering perspective [Mackie and Stojadinović, 2001]. Practicality is determined by the coefficient b (i.e. the slope of the regression line) in the PSDM’s linear regression on a logarithmic scale, as indicated in equation (4). The lower the coefficient b is, the less the IM contributes to the estimation of seismic demand, demonstrating impracticality. As a result, a larger b value denotes a more practical IM.

The practicalities of the IMs are depicted in Fig. 13. The comparisons

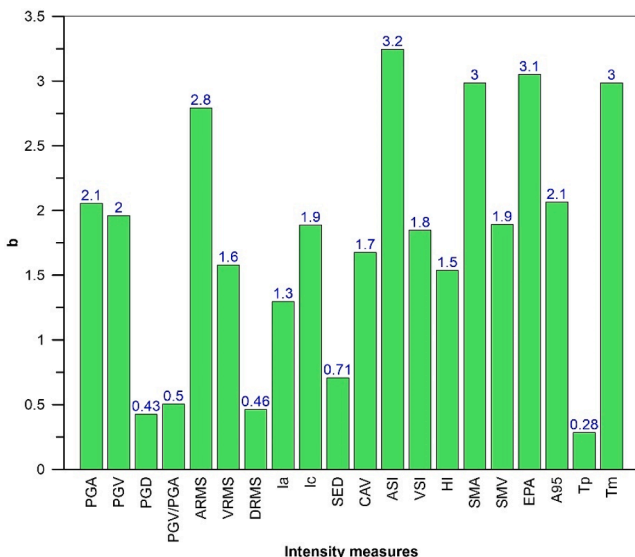


Fig. 13. The b values for practicality.

in Fig. 13 shows that ASI achieved the highest b value ($b = 3.25$) and is the most practical IM. In addition, the greatest practicality is provided by EDA ($b = 3.05$), SMA ($b = 2.99$), and ARMS ($b = 2.79$). T_p has provided the smallest value of coefficient b ($b = 0.2833$), which could indicate its impracticality. PGD ($b = 0.43$), DRMS ($b = 0.46$), and PGV/PGA ($b = 0.50$) are the other least practical IMs.

4.3.4. Proficiency

The proficiency is a criterion that benefits from considering both efficiency and practicability simultaneously [Padgett et al., 2008]. A more proficient IM has less modified dispersion, which highlights the degree of demand uncertainty (EDP) associated with the IM choice. Modified dispersion (ξ), which is derived from equation (8), serves to define proficiency.

$$\xi = \frac{\sigma_{EDP/IM}}{b} \tag{8}$$

A low value of modified dispersion (ξ) indicates more proficient IM. The proficiencies of the IMs (indicated by a lower ξ value) are presented in Fig. 14. By investigating the data for the modified dispersion (ξ), it is observed that EDA ($\xi = 0.20$) has the lowest value among other IMs. VSI ($\xi = 0.21$), SMA ($\xi = 0.22$), ARMS ($\xi = 0.24$) PGV ($\xi = 0.26$) and I_c ($\xi = 0.30$) have modified dispersion (ξ) value close to zero among other IMs. Investigating the IMs proficiency demonstrates that the value of modified dispersion (ξ), for the T_p ($\xi = 5.42$) is the highest, followed by PGD ($\xi = 2.49$), PGV/PGA ($\xi = 2.44$) and DRMS ($\xi = 2.44$).

Based on the investigation for optimal IM selection criteria conducted so far, it is highlighted that the EDA, SMA, ARMS, PGV, and I_c are best earthquake intensity measures correlating with the seismic response of dam settlement. PGA, VRMS, ASI, VSI HI, and I_a show moderate correlation with the damage of the crest settlement. In contrast, PGD, PGV/PGA, and T_p are the weakest correlated with the settlement of the dam crest. According to the results among the scalar intensity measures, EDA is the best correlated with the seismic response of the dam.

5. Seismic fragility assessment

The stability and seismic performance analysis of the dam is crucial to predict damage and minimize potential loss. To evaluate the seismic fragility of dams, it is necessary to define the damage index and specific threshold values based on measurable data or expert opinions. In the seismic damage prediction and post-earthquake assessment for dams,

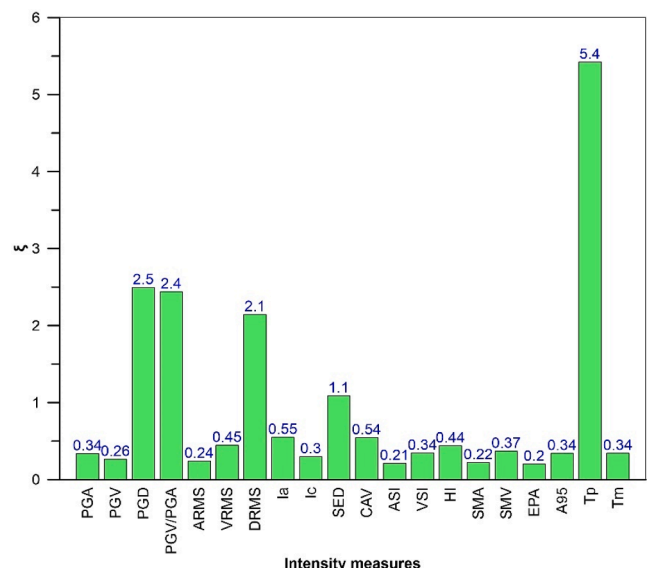


Fig. 14. The ξ values for proficiency.

many researchers have defined the limit states to quantitatively assess the degree of seismic damage.

Pang et al. (2018b) considered the relative settlement of the dam crest and established three limit states: minor (0.2%), moderate (0.4%), and severe (0.6%). Swaisgood (2003) used the data from 69 dams and divided the seismic damage into four states: healthy (<0.1%), minor (0.012–0.5%), moderate (0.1–1.0%), and severe (>0.5%). Swaisgood (2003) considered the relative crest settlement ratio as the assessment index. Pang et al. (2018a) established three limit states based on the settlement ratio of the dam crest. The minor hazard level is specified if the settlement ratio exceeds 0.4%. Similarly, moderate and severe hazard levels are established if the settlement ratio goes beyond 0.7% and 1.0%. In this study, referring to the related literatures of the failure grading of concrete face rockfill dam, the related safety assessment

established by Pells and Fell (2002) is used. The Pells and Fell (2002) damage index includes six different damage states ranging from no or slight to collapse states. These six damage states correspond with maximum relative crest settlement, with no or slight (<0.03%), minor (0.03–0.2%), moderate (0.2–0.5%), major (0.5–1.5%), severe (1.5–5%) and collapse (>5%).

Seismic fragility curves can give results of dam performance evaluation that are more precise and efficient. The seismic fragility curves are produced through the fragility function of the PSDM, as presented in the section 5. The fragility function is depicted in equation (6), in which EDP represents a limit state. The limit values discussed earlier will be used for the generation of fragility curves. This study investigated optimal IMs; EDA, SMA, ARMS, PGV, and I_c are used for the generation of fragility curves. SMA, ARMS, and I_c are more advanced IMs, which are identified

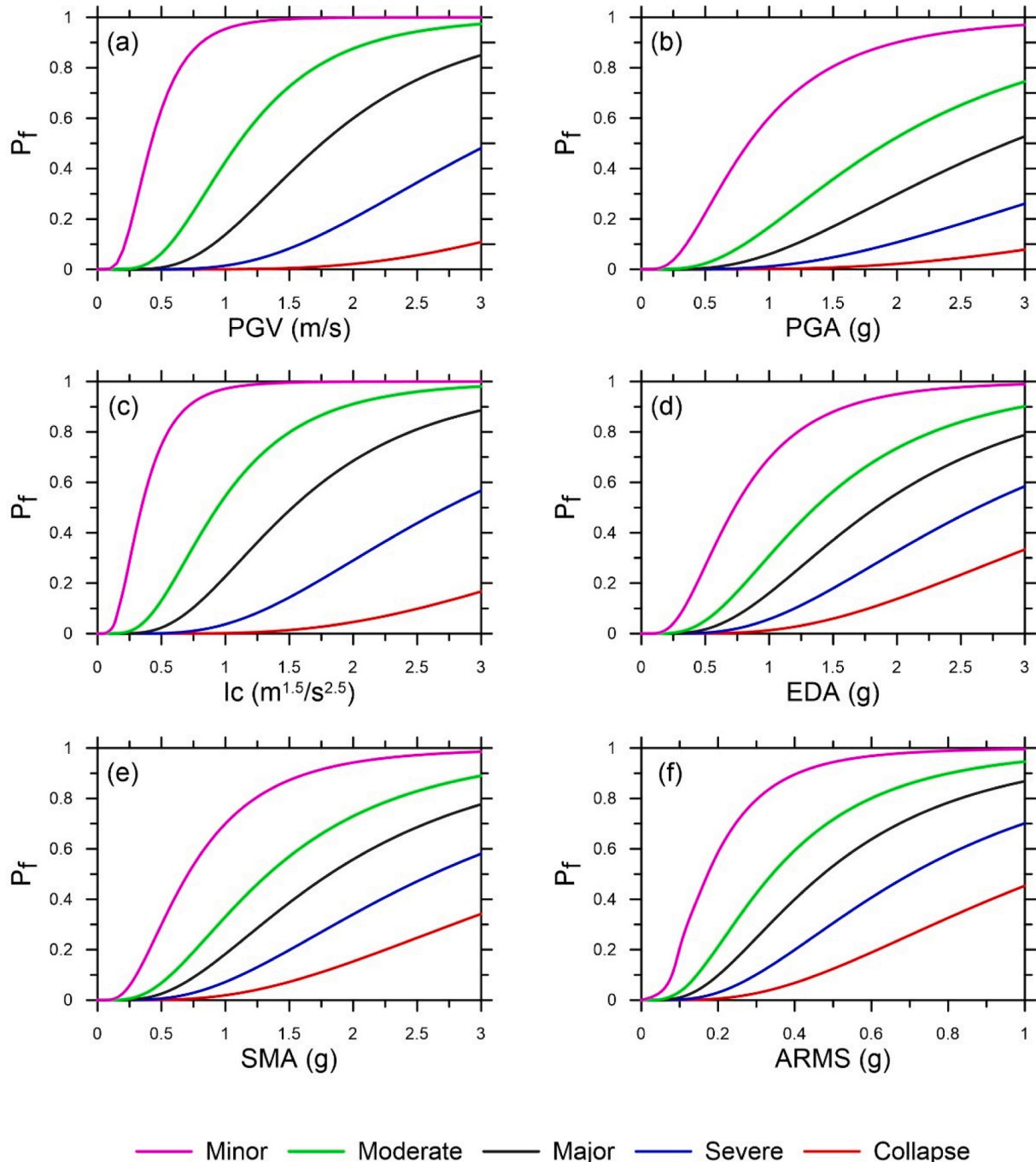


Fig. 15. Seismic fragility curves with respect to (a) PGV (b) PGA (c) I_c (d) EDA (e) SMA (f) ARMS.

as the acceleration-based IMs [Catbas and Aktan, 2002; Nuttli (1979); Vanmarcke and Lai, 1980]. In addition, EDA is computed from response spectra [Kurama and Farrow, 2003]. In the simplest IM, PGV is the maximum absolute value calculated directly from the acceleration.

Fig. 15 presents the seismic fragility curves for the settlement ratio EDP against optimal IMs (EDA, SMA, ARMS, PGV, and I_c). The fragility curve for PGA, which is the most common intensity measure used, is also developed in this study. The generated seismic fragility curves can be used to evaluate the seismic vulnerability of the dam. The probability of failure from a specific damage index can be obtained from single IMs fragility curves. Under the minor damage index ($DI = 0.03\%$), the probabilities of minor failure for the dam are 0.16% at $PGV = 0.25$ m/s, 0.64% at $PGV = 0.50$ m/s and 0.87% at $PGV = 0.75$ m/s, respectively. Meanwhile, it can be noticed that the probabilities for collapse ($DI = 5\%$) are much lower than the minor at the same PGV values. For example, the probability of collapse of a dam is approximately 0.0001% at $PGV = 0.75$ m/s.

The two intensity measure seismic fragility surfaces are also developed. For the estimation of seismic demand in the probabilistic analysis, dual IMs have many benefits over a single IM. The key benefit of two IMs seismic fragility surfaces over a single fragility curve is the fluctuation of system fragility when a second seismic parameter is considered in the probabilistic analysis. In the previous section, it observes that the probability of exceedance may vary depending on the chosen single IM. The PDSM for two IMs can be shown as follows [Jafarian and Miraei, 2019]:

$$\ln(EDP) = b_1 + b_2 \cdot \ln(IM_1) + b_3 \cdot \ln(IM_2) \quad (9)$$

The standard deviation of dual IMs is calculated by equation (9), where the regression coefficient of the model are b_1 , b_2 , and b_3 , and IM_1 and IM_2 represent the two intensity measures.

The scalar optimal IM has disadvantages in demonstrating an adequate relationship between deformation and ground motion and reducing the standard deviation. To achieve a good relationship with deformation, the optimal dual IMs must have an optimum mix of the

goodness of fit, practicality, efficiency, and proficiency. PGA and PGV, PGV, and I_c are selected for the probabilistic vector analysis. Although PGA is not the best scalar IM, it is nevertheless utilized as the second scalar IM since it is the most extensively used IM.

The scatter in the data is significantly reduced with the use of two IMs, and standard deviation is reduced significantly. Fig. 16 depicts the seismic fragility surfaces of different damage indices against the variation of PGA and PGV, and Fig. 17 shows the variation of PGV and I_c . These surfaces can provide a better perspective of the probability of failure compared to fragility curves. To further investigate how the probability of failure is affected by dual IMs, we compared the probability of minor failure with the constant second IM parameter PGA. A significant difference is found to directly make comparisons in the results of fragility curves, considering the constant second IM parameter. Under the minor damage index ($DI = 0.03\%$), the probabilities of minor failure for the dam, at $PGV = 0.50$ m/s, and four different values of PGA 0.25 g, 0.50 g, 0.75 g, and 1.0 g, are 0.07 %, 0.47 %, 0.77 %, and 0.91 %, respectively. These results demonstrate that the dual fragility surfaces can predict the dam failure probability accurately.

6. Verification of developed fragility curves

In this section, a comparison is made with the documented case studies of concrete face rock fill dams for the verification of developed numerical fragility curves. Damage is reported for the Cogswell dam in California due to an earthquake. The earthquake occurred on 17th January 1994 with a magnitude of 6.7 resulted in a relative crest settlement of 0.02 %. This measured relative settlement corresponds with no or slight damage in our study. The bedrock peak ground acceleration measured during the earthquake was 0.11 g [Swaisgood, 2013]. The probability of minor failure from a PGA of 0.11 g is 0.00323 %, which shows that the dam has no or slight damage.

For further verification of developed numerical fragility curves, the present study fragility results are compared with measured data of the Zipingpu dam in China. The Zipingpu dam suffered substantial

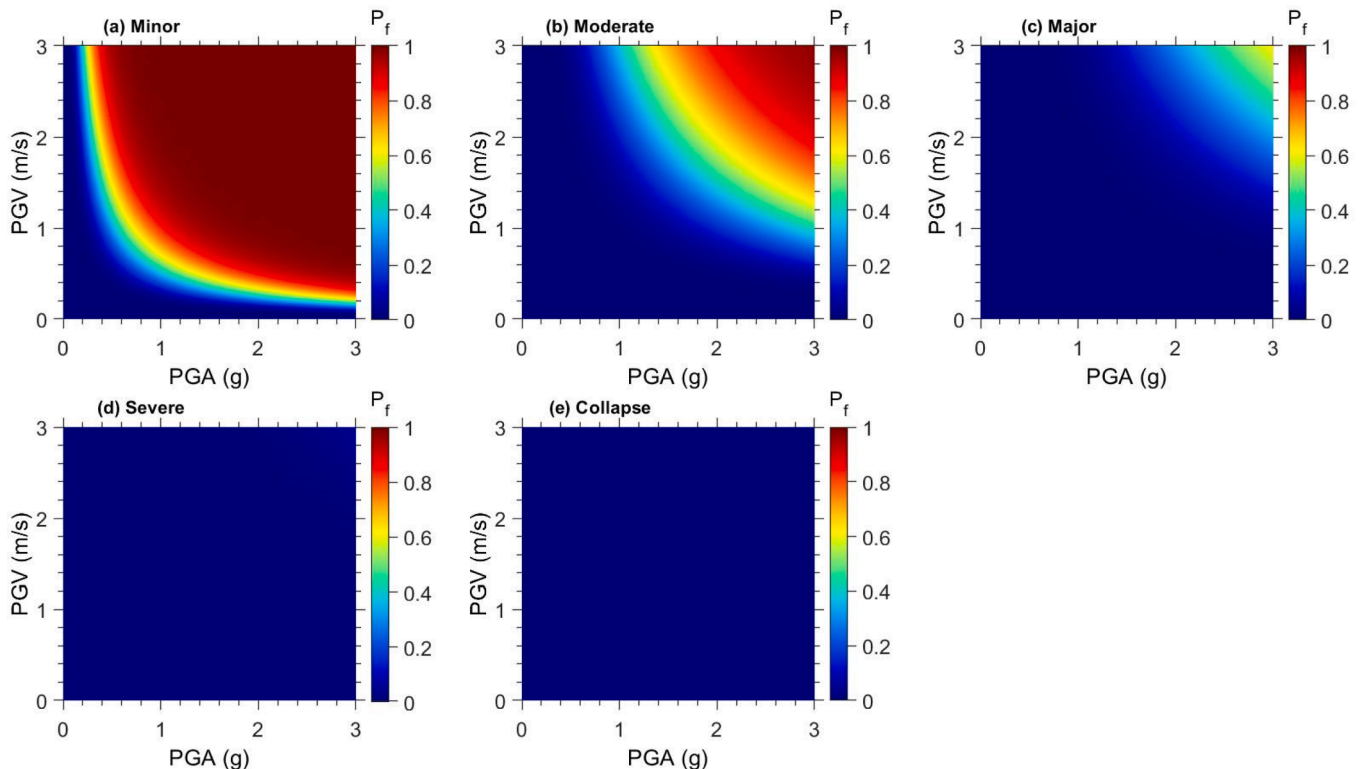


Fig. 16. Seismic fragility surfaces with respect to the two intensity measures (PGA and PGV) (a) Minor (b) Moderate (c) Major (d) Severe (e) Collapse.

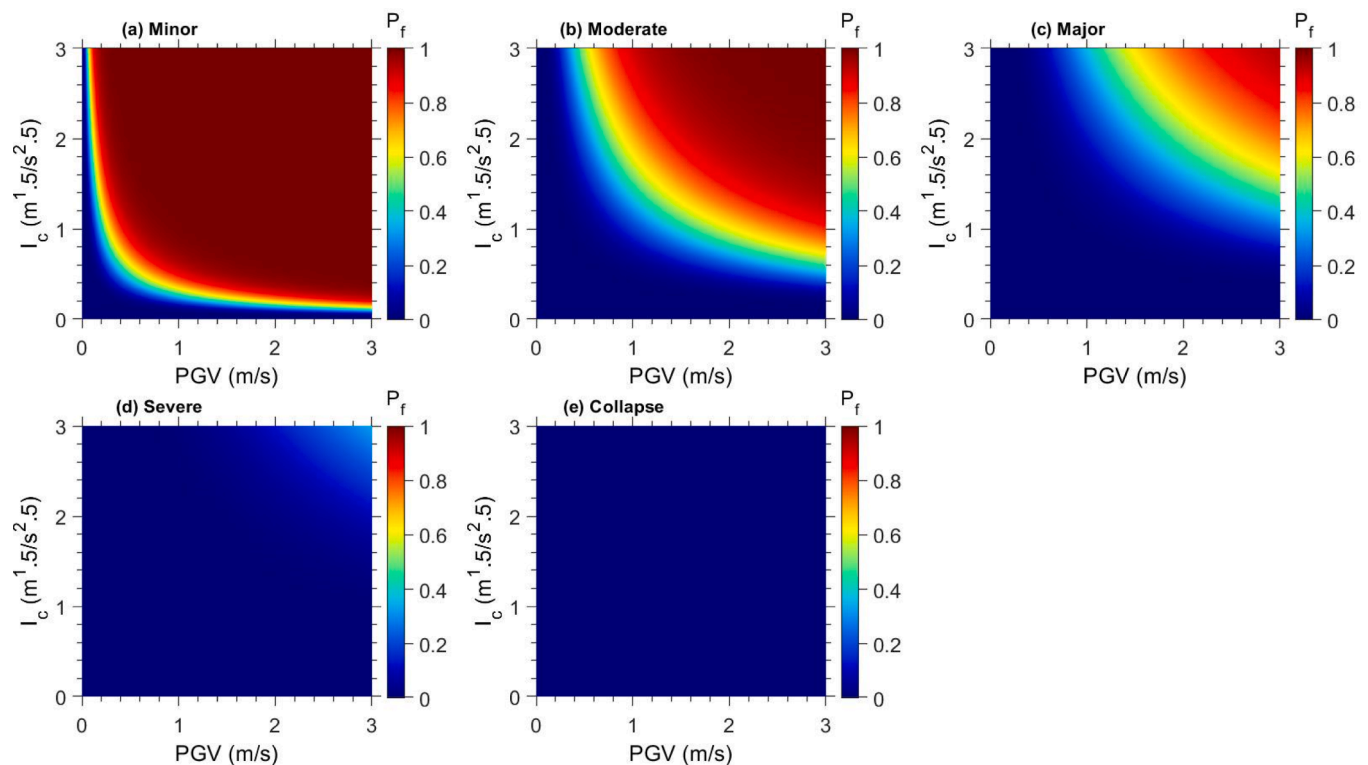


Fig. 17. Seismic fragility surfaces with respect to the two intensity measures (PGV and I_c) (a) Minor (b) Moderate (c) Major (d) Severe (e) Collapse.

deformation and crest settlement during the Wenchuan earthquake that occurred on 12th May 2008 [Kong et al., 2010]. The earthquake caused a relative settlement of 0.48% for the Zippingpu dam [Chen and Han, 2009; Zou et al., 2013]. The acceleration time history at the crest of the slope was recorded by a seismograph with a PGA of 2.06 g [Zhang et al., 2015]. According to damage states defined in the previous section, the relative settlement of 0.48 % corresponds to the moderate damage state. The probability of moderate and minor failure from a PGA of 2.06 g is 0.532 % and 0.907 %, respectively. Due to the lack of acceleration time history data to calculate intensity measures, only PGA is considered in the comparison to validate the current study. The comparison shows that the developed fragility curves can depict the seismic vulnerability of concrete face rock fill dams.

7. Conclusions

Dams are critical facilities used for water storage and electricity generation. In recent decades, the performance-based earthquake engineering of multifunctional facilities like dams has been given more attention by earthquake engineering professionals to ensure their safety. The development of seismic fragility curves for the evaluation of the seismic performance of a dam is a popular approach using IMs and damage states. The main sources of uncertainty for assessing the seismic performance of a dam are soil properties and IMs.

The 2D nonlinear dynamic finite element model was used to calculate the seismically induced crest settlement of dams. Prior to performing the analyses, the numerical model was validated against centrifuge measurements. The geometry of the dam and shear wave velocity were determined based on the average values used for dams in South Korea. The optimal seismic intensity measures (IMs) for dam fragility curves and developed seismic fragility surfaces were evaluated using dual intensity measures. Four selection criteria were used to assess the optimal intensity measure: the goodness of fit, practicality, efficiency and proficiency.

- Among the 20 IMs tested, it is highlighted that the EDA, SMA, ARMS, PGV, and I_c provide the most favorable predictions for the seismic assessment of dam performance. However, the widely used PGA is demonstrated not to be one of the optimal IMs according to the criteria used in the study.
- Based on the results of optimal intensity measures and nonlinear dynamic analyses, the scalar seismic fragility curves for optimal IMs are developed. Fragility curves for PGA, which is the most widely used IM, are also established.
- The results of dual intensity measure fragility curves can better describe the seismic performance of the dam compared with single IM-based curves because the use of an additional IM reduces the scatter in the data and also increases the correlation.
- The single IM-based fragility curves and dual IM conditioned surfaces are shown to display significant differences, implying that using scalar IMs to develop fragility curves should be utilized with caution. Furthermore, the single IM fragility curve tends to underestimate or overstate the hazard. Finally, the dam damage can be analyzed using the fragility curves created for EDP and IMs. Furthermore, to increase the correlation and validity between seismic IMs parameters and EDP, the dual IMs analysis approach is recommended to be used in a probabilistic seismic demand analysis.

CRediT authorship contribution statement

Muhammad Irsilan Khalid: Investigation, Software, Writing – original draft, Writing – review & editing, Visualization. **Duheer Park:** Conceptualization, Methodology, Writing – review & editing. **Jianbo Fei:** Conceptualization, Methodology, Writing – review & editing, Project administration. **Van-Quang Nguyen:** Writing – original draft, Methodology, Writing – review & editing. **Duy-Duan Nguyen:** Writing – review & editing. **Xiangsheng Chen:** Supervision, Funding acquisition.

Declaration of Competing Interest

The authors declare that they have no known competing financial interests or personal relationships that could have appeared to influence the work reported in this paper.

Data availability

Data will be made available on request.

Acknowledgment

The research is funded by the National Natural Science Foundation of China (Grants No. 52178339, 52090081 and 52008261) and Shenzhen Natural Science Fund (the Stable Support Plan Program 20220808150117002).

References

- Arias, A., 1970. A measure of earthquake intensity. Seismic Design for Nuclear Power Plants, Massachusetts Institute of Technology.
- Baeg, J., Park, D., Yoon, J., Choi, B.-H., 2018. Evaluation of seismic fragility of concrete faced rockfill dam. *J Korean Geosynth* 17 (4), 103–108.
- Benjamin, J.R., 1988. A criterion for determining exceedances of the operating basis earthquake, Epr report np-5930. Electric Power Research Institute, Palo Alto.
- Bolisetti, C., Whittaker, A.S., Coleman, J.L., 2018. Linear and nonlinear soil-structure interaction analysis of buildings and safety-related nuclear structures. *Soil Dyn. Earthq. Eng.* 107, 218–233.
- Catbas, F.N., Aktan, A.E., 2002. Condition and damage assessment: Issues and some promising indices. *J. Struct. Eng.* 128 (8), 1026–1036.
- Chen, S.-S., Han, H.-Q., 2009. Impact of the '5.12' Wenchuan earthquake on Zipingpu concrete face rock-fill dam and its analysis. *Geomechanics and Geoengineering: An International Journal* 4 (4), 299–306.
- Cooke, J.B., 1992. Development of the high concrete faced rockfill dam. *Int Water Power Dam Constr* 44 (4), 7–10.
- Cornell, C.A., Jalayer, F., Hamburger, R.O., Foutch, D.A., 2002. Probabilistic basis for 2000 SAC federal emergency management agency steel moment frame guidelines. *J. Struct. Eng.* 128 (4), 526–533.
- Darendeli, M.B., 2001. Development of a new family of normalized modulus reduction and material damping curves. University of Texas at Austin, Texas, USA [Ph.D. Thesis].
- Giovenale, P., Cornell, C.A., Esteve, L., 2004. Comparing the adequacy of alternative ground motion intensity measures for the estimation of structural responses. *Earthq. Eng. Struct. Dyn.* 33 (8), 951–979.
- Groholski, D.R., Hashash, Y.M.A., Kim, B., Musgrove, M., Harmon, J., Stewart, J.P., 2016. Simplified model for small-strain nonlinearity and strength in 1D seismic site response analysis. *J Geotech Geoenviron* 142 (9), 04016042.
- Guo, J., Alam, M.S., Wang, J., Li, S., Yuan, W., 2020. Optimal intensity measures for probabilistic seismic demand models of a cable-stayed bridge based on generalized linear regression models. *Soil Dyn. Earthq. Eng.* 131, 106024.
- Hariri-Ardebili, M., Saouma, V., 2016. Probabilistic seismic demand model and optimal intensity measure for concrete dams. *Struct. Saf.* 59, 67–85.
- Hashash, Y.M.A., Dashti, S., Musgrove, M., Gillis, K., Walker, M., Ellison, K., et al., 2018. Influence of tall buildings on seismic response of shallow underground structures. *J Geotech Geoenviron* 144 (12), 04018097.
- Housner, G., Jennings, P.C., 1964. Generation of artificial earthquakes. *J ENG MECH DIV-ASCE* 90 (1), 113–150.
- Housner, G. W. 1952. Spectrum intensities of strong-motion earthquakes.
- Hu, Z., Wei, B., Jiang, L., Li, S., Yu, Y., Xiao, C., 2022. Assessment of optimal ground motion intensity measure for high-speed railway girder bridge (HRGB) based on spectral acceleration. *Eng. Struct.* 252, 113728.
- Hu, X., Zhou, Z., Chen, H., Ren, Y., 2020. Seismic fragility analysis of tunnels with different buried depths in a soft soil. *Sustain* 12 (3), 892.
- Huang, Z.-K., Ptilakis, K., Argyroudis, S., Tsinidis, G., Zhang, D.-M., 2021. Selection of optimal intensity measures for fragility assessment of circular tunnels in soft soil deposits. *Soil Dyn. Earthq. Eng.* 145, 106724.
- Huang, X., Shengjie, D., Lu, X., Miao, Z., Huang, P., 2023. Numerical simulation study on dynamic characteristics of high concrete faced sandy gravel dam. In: *Advances in Civil Engineering: Structural Seismic Resistance*. CRC Press, Monitoring and Detection, pp. 39–44.
- Jafarian, Y., Miraei, M., 2019. Scalar-and vector-valued fragility analyses of gravity quay wall on liquefiable soil: Example of Kobe Port. *Int. J. Geomech.* 19 (5), 04019029.
- Kazantzi, A.K., Vamvatsikos, D., 2015. Intensity measure selection for vulnerability studies of building classes. *Earthq. Eng. Struct. Dyn.* 44 (15), 2677–2694.
- Khalid, M.I., Lee, Y., Lee, Y., Kim, H.-S., Park, D., 2021a. Effect of characteristics of ground motion on seismically induced sliding surface of slopes. *Appl. Sci.* 11 (12), 5319.
- Khalid, M.I., Pervaiz, U., Park, D., 2021b. Investigation of effect of input ground motion on the failure surface of mountain slopes. *Journal of the Korean GEO-environmental Society* 22 (7), 5–12.
- Kim, M.-K., Lee, S.-H., Choo, Y.W., Kim, D.-S., 2011. Seismic behaviors of earth-core and concrete-faced rock-fill dams by dynamic centrifuge tests. *Soil Dyn. Earthq. Eng.* 31 (11), 1579–1593.
- Kong, X.-j., Zhou, Y., Xu, B., Zou, D.-g. 2010. Analysis on seismic failure mechanism of Zipingpu dam and several reflections of aseismic design for high rock-fill dam. *Earth and Space 2010: Engineering, Science, Construction, and Operations in Challenging Environments* 3177–89.
- Kostinakis, K., Athanatopoulou, A., Morfidis, K., 2015. Correlation between ground motion intensity measures and seismic damage of 3D R/C buildings. *Eng. Struct.* 82 (151–67).
- Kramer, S.L., 1996. *Geotechnical Earthquake Engineering*. Prentice-Hall, Upper Saddle River, NJ, USA.
- Kuhlemeyer, R.L., Lysmer, J., 1973. Finite element method accuracy for wave propagation problems. *J. Soil Mech. Found. Div.* 99 (Tech Rpt).
- Kurama, Y., Farrow, K., 2003. Ground motion scaling methods for different site conditions and structure characteristics. *Earthq. Eng. Struct. Dyn.* 32 (15), 2425–2450.
- Lee, S., Kim, B., Lee, Y.-J., 2019. Seismic fragility analysis of steel liquid storage tanks using earthquake ground motions recorded in Korea. *Math Probl Eng.* 1–15.
- Lee, Y., Kim, H.-S., Khalid, M.I., Lee, Y., Park, D., 2020. Effect of nonlinear soil model on seismic response of slopes composed of granular soil. *Adv Civ Eng.*
- Li, Z., Wu, Z., Chen, J., Pei, L., Lu, X., 2021. Fuzzy seismic fragility analysis of gravity dams considering spatial variability of material parameters. *Soil Dyn. Earthq. Eng.* 140, 106439.
- Li, Z., Wu, Z., Lu, X., Zhou, J., Chen, J., Liu, L., et al., 2022. Efficient seismic risk analysis of gravity dams via screening of intensity measures and simulated non-parametric fragility curves. *Soil Dyn. Earthq. Eng.* 152, 107040.
- Li, C., Zhai, C., Kunmath, S., Ji, D., 2019. Methodology for selection of the most damaging ground motions for nuclear power plant structures. *Soil Dyn. Earthq. Eng.* 116, 345–357.
- Liang, H., Tu, J., Guo, S., Liao, J., Li, D., Peng, S., 2020. Seismic fragility analysis of a High Arch Dam-Foundation System based on seismic instability failure mode. *Soil Dyn. Earthq. Eng.* 130, 105981.
- LSTC. 2007. *LS-DYNA Theory Manual*.
- Lu, D., Liu, Y., Yu, X., Huang, M., 2015. Probabilistic seismic demand models and fragility analysis of RC continuous girder bridges. *Symposium on Reliability of Engineering System (SRES'2015)*.
- Ma, H., Chi, F., 2016. Technical progress on researches for the safety of high concrete-faced rockfill dams. *Engineering* 2 (3), 332–339.
- Macabuag, J., Rossetto, T., Ioannou, I., Suppasri, A., Sugawara, D., Adriano, B., et al., 2016. A proposed methodology for deriving tsunami fragility functions for buildings using optimum intensity measures. *Nat. Hazards* 84, 1257–1285.
- Mackie, K., Stojadinović, B., 2001. Probabilistic seismic demand model for California highway bridges. *J. Bridg. Eng.* 6 (6), 468–481.
- Mahmoodi, K., Noorzad, A., Mahboubi, A., Alembagheri, M., 2021. Seismic performance assessment of a cemented material dam using incremental dynamic analysis. *Elsevier, Struct.*, pp. 1187–1198.
- Nguyen, D.-D., Thusa, B., Han, T.-S., Lee, T.-H., 2020. Identifying significant earthquake intensity measures for evaluating seismic damage and fragility of nuclear power plant structures. *Nucl. Eng. Technol.* 52 (1), 192–205.
- Nguyen, D.-D., Lee, T.-H., Phan, V.-T., 2021. Optimal earthquake intensity measures for probabilistic seismic demand models of base-isolated nuclear power plant structures. *Energies* 14 (16), 5163.
- Nguyen, H.D., Shin, M., LaFave, J.M., 2023. Optimal intensity measures for probabilistic seismic demand models of steel moment frames. *J Build Eng* 65, 105629.
- Nuttli, O. W. 1979. The relation of sustained maximum ground acceleration and velocity to earthquake intensity and magnitude: US Army Engineer Waterways Experiment Station.
- Padgett, J.E., Nielson, B.G., DesRoches, R., 2008. Selection of optimal intensity measures in probabilistic seismic demand models of highway bridge portfolios. *Earthq. Eng. Struct. Dyn.* 37 (5), 711–725.
- Pang, R., Xu, B., Kong, X., Zhou, Y., Zou, D., 2018a. Seismic performance evaluation of high CFRD slopes subjected to near-fault ground motions based on generalized probability density evolution method. *Eng. Geol.* 246, 391–401.
- Pang, R., Xu, B., Kong, X., Zou, D., 2018b. Seismic fragility for high CFRDs based on deformation and damage index through incremental dynamic analysis. *Soil Dyn. Earthq. Eng.* 104, 432–436.
- Pang, R., Xu, B., Zhou, Y., Zhang, X., Wang, X., 2020. Fragility analysis of high CFRDs subjected to mainshock-aftershock sequences based on plastic failure. *Eng. Struct.* 206, 110152.
- Park, Y.-J., Ang, A.-H.-S., Wen, Y.K., 1985. Seismic damage analysis of reinforced concrete buildings. *J Struct Eng (N Y N Y)* 111 (4), 740–757.
- Pejovic, J.R., Serdar, N.N., Pejovic, R.R., 2017. Optimal intensity measures for probabilistic seismic demand models of RC high-rise buildings. *Earthq Struct* 13 (3), 221–230.
- Pejovic, J.R., Serdar, N.N., Pejovic, R.R., 2018. Novel optimal intensity measures for probabilistic seismic analysis of RC high-rise buildings with core. *Earthq Struct* 15 (4), 443–452.
- Pells, S., Fell, R., 2002. Damage and cracking of embankment dams by earthquakes and the implications for internal erosion and piping. University of New South Wales, School of Civil and Environmental Engineering.
- Rathje, E.M., Abrahamson, N.A., Bray, J.D., 1998. Simplified frequency content estimates of earthquake ground motions. *J. Geotech. Geoenviron. Eng.* 124 (2), 150–159.
- Rong, X.-L., Yang, J.-H., Jun, L., Zhang, Y.-X., Zheng, S.-S., Dong, L., 2023. Optimal ground motion intensity measure for seismic assessment of high-rise reinforced concrete structures. *Case Stud. Constr. Mater.* 18, e01678.

- Sarma, S., Yang, K., 1987. An evaluation of strong motion records and a new parameter A95. *Earthq. Eng. Struct. Dyn.* 15 (1), 119–132.
- Segura, R., Padgett, J.E., Paultre, P., 2020. Metamodel-based seismic fragility analysis of concrete gravity dams. *J. Struct. Eng.* 146 (7), 04020121.
- Seismosoft, L., 2012. *SeismoSignal*. Pavia, Italy.
- Sevieri, G., De Falco, A., Andreini, M., Matthies, H.G., 2021. Hierarchical Bayesian framework for uncertainty reduction in the seismic fragility analysis of concrete gravity dams. *Eng. Struct.* 246, 113001.
- Shannon, D. A. 2009. Dam damage: Evaluating and learning from the Wenchuan earthquake's impact to China's dams. *TCLÉE 2009: Lifeline Earthquake Engineering in a Multihazard Environment* 1–12.
- Sun, B., Deng, M., Zhang, S., Wang, C., Du, M., 2022. Seismic performance assessment of high asphalt concrete core rockfill dam considering shorter duration and longer duration. *Elsevier, Struct. pp.* 1204–1217.
- Sun, B., Deng, M., Zhang, S., Wang, C., Cui, W., Li, Q., et al., 2023. Optimal selection of scalar and vector-valued intensity measures for improved fragility analysis in cross-fault hydraulic tunnels. *Tunn Undergr. Space Technol* 132, 104857.
- Swaigood, J. 2003. Embankment dam deformations caused by earthquakes. *The 2003 Pacific conference on earthquake engineering*. Christchurch, New Zealand.
- Swaigood, J. Predicting dam deformation caused by earthquakes-an update. 2013. *Annual Conference Proceedings—Association of State Dam Safety Officials Incorporated*, New York 970–80.
- Tidke, A.R., Adhikary, S., 2021. Seismic fragility analysis of the Koyna gravity dam with layered rock foundation considering tensile crack failure. *Eng. Fail. Anal.* 125, 105361.
- Vanmarcke, E.H., Lai, S.-S.-P., 1980. Strong-motion duration and RMS amplitude of earthquake records. *Bull. Seismol. Soc. Am.* 70 (4), 1293–1307.
- Wang, J.-T., Zhang, M.-X., Jin, A.-Y., Zhang, C.-H., 2018. Seismic fragility of arch dams based on damage analysis. *Soil Dyn. Earthq. Eng.* 109, 58–68.
- Wei, B., Hu, Z., He, X., Jiang, L., 2020. Evaluation of optimal ground motion intensity measures and seismic fragility analysis of a multi-pylon cable-stayed bridge with super-high piers in mountainous areas. *Soil Dyn. Earthq. Eng.* 129, 105945.
- Xing, H.-F., Gong, X.-N., Zhou, X.-G., Fu, H.-F., 2006. Construction of concrete-faced rockfill dams with weak rocks. *J. Geotech Geoenviron* 132 (6), 778–785.
- Xu, B., Wang, X., Pang, R., Zhou, Y., 2022. Effect of multi-components strong motion duration on seismic performance of high CFRDs based on fragility analysis. *J Earthq Eng* 1–19.
- Xu, Z. Performance of Zipingpu CFRD during the strong earthquake. 2008. *Proceedings of 10th Intern Symposium on Landslides and Engineered Slopes* 481–96.
- Yamaguchi, Y., Iwashita, T., Mitsuishi, S., 2008. Preliminary investigation of dams stricken by the Iwate-Miyagi Nairiku Earthquake in 2008. 2008. *Proceedings of the fifth east Asian regional dam conference international symposium on co-existence of environment and dams*.
- Zelaschi, C., Monteiro, R., Pinho, R., 2019. Critical assessment of intensity measures for seismic response of Italian RC bridge portfolios. *J. Earthq. Eng.* 23 (6), 980–1000.
- Zhang, J., Huo, Y., 2009. Evaluating effectiveness and optimum design of isolation devices for highway bridges using the fragility function method. *Eng. Struct.* 31 (8), 1648–1660.
- Zhang, J.-M., Yang, Z.-Y., Gao, X.-Z., Tong, Z.-X., 2010. Lessons from damages to high embankment dams in the May 12, 2008 Wenchuan earthquake. *Soil Dyn Earthq Eng* 1–31.
- Zhang, J.-M., Yang, Z., Gao, X., Zhang, J., 2015. Geotechnical aspects and seismic damage of the 156-m-high Zipingpu concrete-faced rockfill dam following the Ms 8.0 wenchuan earthquake. *Soil Dyn. Earthq. Eng.* 76, 145–156.
- Zhou, Y., Zhang, Y., Pang, R., Xu, B., 2021. Seismic fragility analysis of high concrete faced rockfill dams based on plastic failure with support vector machine. *Soil Dyn. Earthq. Eng.* 144, 106587.
- Zou, D., Xu, B., Kong, X., Liu, H., Zhou, Y., 2013. Numerical simulation of the seismic response of the zipingpu concrete face rockfill dam during the wenchuan earthquake based on a generalized plasticity model. *Comput. Geotech.* 49, 111–122.

